

Seismic Response Prediction of Spatial Base-Isolated Structures

Donatello Cardone¹, Andrea Lucchini², Emanuele Mastrangelo³,
Fabrizio Mollaioli⁴

^{1,3}School of Engineering, University of Basilicata, Via dell'Ateneo Lucano 10, I- 85100 Potenza, Italy

^{2,4}Department of Structural and Geotechnical Engineering, Sapienza University of Rome,
Via Gramsci 53, I-00197 Rome, Italy

Abstract

Several methods can be found in the literature for the selection and scaling of ground motion records to be used in the seismic response history analysis of structures. These methods make use of a parameter, called intensity measure, for quantifying the intensity level of the earthquake and selecting and scaling the records. In this study, alternative intensity measures are evaluated with respect to the seismic response prediction of base-isolated buildings. The predictive efficiency of the intensity measures is estimated from the regression of responses obtained from a cloud analysis. The case-study selected for the analysis is a reinforced concrete frame building originally designed for gravity loads only and then retrofitted by seismic isolation. Two different isolation systems are examined. A comprehensive set of seismic ground motions, including both ordinary and pulse-like near-fault records, is used in the analysis.

Keywords: Base-isolated Buildings, Seismic Response Prediction, Intensity Measure

1. Introduction

Much research has been spent to investigate the capability of seismic intensity measures (IMs) to predict the response of fixed-base structures (e.g., [1], [2], and [3]). Few studies, however, have focused on base-isolated structures [4].

Generally, the most widely investigated IMs are the peak ground acceleration (PGA) and the spectral acceleration at the fundamental period of the structure ($S_a(T_1)$), because of the large number of hazard curves available in the literature. Nonetheless, for tall and long-period buildings as well as for structures subjected to near-source ground motions, $S_a(T_1)$ may not be a good predictor because of the limited spectral shape information (see [5] and [6]). This is in part due to the fact that $S_a(T_1)$ accounts neither for contribution of higher modes nor for period lengthening caused by structural nonlinearity. Several alternative IMs were proposed as multiplicative adjustments of $S_a(T_1)$ in order to explicitly overcome the aforementioned drawbacks ([5]; [7]; [6]; [2]; [8]). The

objective of these proposals was not only to improve the predictive efficiency of the IM for all damage levels of a given structure, but also to account for the IM computability through a ground-motion hazard analysis without the need of any new attenuation relationships. Moreover, numerous spectrum-based scalar IMs including energy-derived ones were investigated, and studies showed that velocity-based IMs are in general better correlated to deformation demands especially in the case of medium-rise frame structures. Some authors ([3], [9], [10], [11]) showed that the peak ground velocity (PGV) is in general an effective IM for predicting the response of base-isolated structures. Also, it was demonstrated that the predictions using this scalar IM can be significantly improved by considering a vector IM that includes, in addition to the PGV, also the PGA, and the following parameters: I_a , E_v and PD , as defined in [12], [13], and [14], respectively. This study aims at investigating the predictive capability of a large number of scalar IMs by taking into account both ordinary and pulse-like near fault ground motions. In order to achieve this goal, the efficiency of the considered IMs is estimated through regression analyses of responses obtained using a database of records consisting of 72 ordinary and 20 pulse-like ground motions. The nonlinear dynamic analyses are carried out on a 6-storey frame concrete building, originally designed for gravity loads only, and then retrofitted by seismic isolation. The engineering demand parameters (EDPs) considered in this study for measuring the structural demand are the Maximum Inter-storey Drift Ratio (MIDR), the Maximum Floor Acceleration (MFA) and the Maximum Base Displacement (MBD). Only scalar IMs are investigated, since vector IMs are frequently considered to be still not sufficiently practical because of the high evaluation efforts they usually require in the assessment analyses.

2. Case studies

2.1 Description of the analyzed structures

The case-study building is an archetype 6-storey RC residential frame building (see Fig. 1), whose characteristics have been derived through a simulated design considering gravity loads only, according to the Code and state of practice enforced in Italy before the '70s. The plan dimensions of the building are 27.00m and 15.00m, with a floor area approximately equal to 405m².

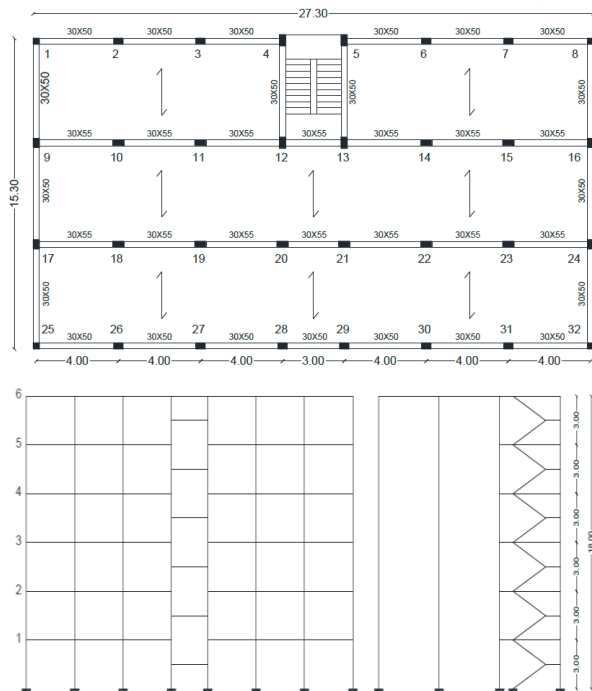


Fig. 1 Plan and elevation view of the frame structure analyzed in the study.

The building height from the ground is 18.00m, with a constant interstorey height equal to 3.00 m. Gravity loads are sustained by four frames oriented along the largest plan dimension of the building. Along the short side, instead, the lateral load-resisting system of the structure consists of two external frames, and two internal frames near located the staircase. All the beams' cross sections are 300×500 mm, except the internal ones oriented along largest plan dimension of the building, which are 300×550 mm. The corner columns have square sections of 300 mm. At the first and second story, dimensions of the external and the internal columns are 300×450 mm and 300×550 mm, respectively; at the third and fourth dimensions change to

300×350 mm and 300×450 mm, while at the fifth and sixth story to 300×300 mm and 300×350 mm.

The allowable-stress method has been adopted to design the steel reinforcement of the structural members, considering smooth steel bars with end hooks at the end of exterior beam-column joints and at the base of the columns. The percentage of longitudinal reinforcement ranges from 0.68 % to 0.75 % for columns, and from 0.56 % to 0.71 % for beams. Transverse reinforcement consists of 6 mm stirrups, with constant spacing equal to 200 mm and 150 mm for columns and beams, respectively.

2.2 Modeling assumptions

The finite element modeling of the structures has been built in OpenSees. The beam/column flexural behavior has been described with beam with plastic hinges elements, modeled using the modified IMK deterioration model with peak-oriented hysteretic response [15]. The skeleton curves of the plastic hinges have been derived from moment-curvature analyses of the critical cross sections, using for concrete and steel the constitutive laws shown in Fig.2a and Fig.2b, respectively.

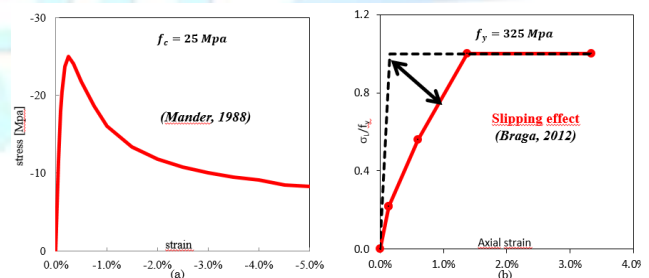


Fig.2(a) Concrete constitutive law and (b) steel rebars constitutive law.

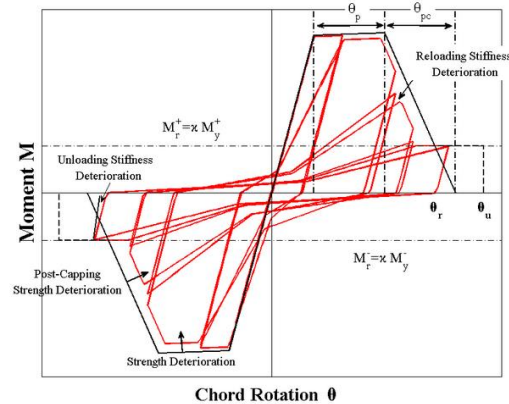


Fig.3 Modified IMK model with pinched hysteretic response [16].

In particular, slipping has been taken into account by adopting for the longitudinal bars a modified constitutive law in tension [17], and neglecting the contribution of the rebars in compression (e.g. [18]; [19]). The moment-

curvature relationship, has been then converted into a tri-linear moment-curvature curve for representing the elastic, post-cracking, post-yielding, post capping behavior (see Fig.3), consistently with the model by [15].

Exterior masonry infills have been modeled with an equivalent compression-only strut model (see Fig.4a), characterized by a bi-linear skeleton curve described by the modifiedDecanini model [20] (see Fig.4b).

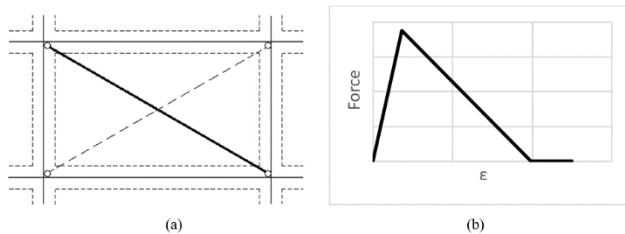


Fig.4 Finite element model for masonry infills:(a) equivalent compression-only strut and (b) adopted skeleton curve.

Two different types of isolation systems have been considered in the study: (i) high damping rubber bearings (HDRBs), under the external columns, + flat sliding bearings (FSBs), under the internal columns; (ii) a system of friction pendulum bearings (FPBs) under all the columns of the structure. Both isolation systems have been designed according to [21].

The model recently developed by [22] has been used to describe the cyclic behavior of the HDRBs. The model consists of a two-node element, connected by six springs that represent the mechanical behavior of the bearing in the internal degrees of freedom of the element (Fig.5).

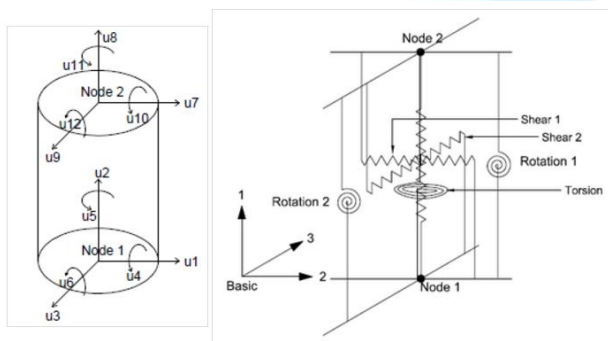


Fig.5 Degrees of freedom and discrete spring representation of the elastomeric bearings [23].

Coupling between the two shear springs is considered explicitly by using a bidirectional model. All the other springs are modeled as uncoupled. In particular, interaction between the vertical and the horizontal constitutive behavior is considered indirectly by using expressions for the mechanical properties in one direction that depend on response parameters in the other direction.

For the torsional and the rotational springs a simplified linear behavior is assumed, as they are not expected to significantly affect the response of the elastomeric bearing. In summary, the following material models have been adopted for the six different springs: the model proposed by [22], which captures the behavior under cyclic tension, for the axial spring; the bidirectional model proposed by [24], for the two shear springs; linear models, for both the torsional and the two rotational springs. It is important to underline that by using this model the following phenomena are represented: scragging effects that produce degradation of stiffness and damping in shear; cavitation and post-cavitation behavior in tension; variation in critical buckling load capacity caused by large lateral displacements; variation in vertical axial stiffness with horizontal displacement. For the FSBs, flat slider bearing elements with no friction resistance have been used. In order to account for possible lifting of the bearing, the uniaxial material adopted in the axial direction has been calibrated so that to have a zero strength in tension.

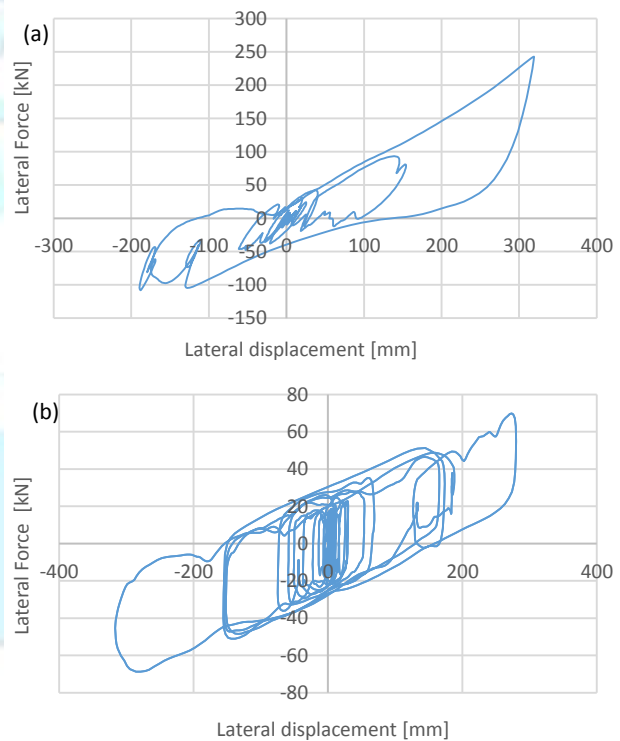


Fig.6 Cyclic behavior representative of (a) the HDRBs and (b) the FPBs.

The cyclic behavior of the FPBs has been modelled using the single friction pendulum bearing element available in OpenSees, which features coupled friction properties for the two shear deformations, post-yielding stiffness in the shear directions (determined from the concave sliding

surface properties), and tension gap in the axial direction to capture the uplift behavior of the bearing. This model is characterized by a hysteretic behavior that depends on the sliding friction coefficient at low (μ_{slow}) and fast (μ_{fast}) sliding velocities, which are velocity- and pressure-dependent, according to the mathematical model proposed by [25]. In this study, μ_{fast} has been set equal to 2.5%, in line with the manufacturer provisions for a design value of the axial load ratio (i.e. the maximum axial load divided by the axial bearing capacity) approximatively equal to 1.0. μ_{slow} has been assumed 1/2.5 times μ_{fast} , according to [26]. Both the isolation systems have been designed following the approach described in [27].

Further details on the numerical models used for the isolation systems and the superstructure can be found in [28] and [29].

Finally, the cyclic behavior representative of the HDRBs and the FPBs is reported in Fig. 6; reported in Table 1 the values of the fundamental periods of vibration of the two base-isolated buildings calculated for the design earthquake intensity level.

Table 1: Fundamental periods of vibration of the base-isolated buildings

Seismic Isolation System	T_{IS}
20HDRB+12FSB	2.90
32FPS	3.40

2.3 Ground motion database

A set of 92 earthquake ground motions (GMs) has been selected from the Next Generation of Attenuation project database [30] and used as input for the nonlinear dynamic analyses of the base-isolated buildings. The above suite of GMs is composed by two groups: ordinary GMs (72 records, with closest distance ranging from 0.34 km to 87.87 km, and moment magnitude from 5.74 to 7.9) and pulse-like near-fault GMs (20 records, with closest distance ranging from 0.34 km to 20.82 km, and moment magnitude from 5.21 to 6.93). The latter are identified as pulse-like by using the method based on the wavelet analysis approach proposed by [31]. All the acceleration-time histories are recorded on soil classified as type C or D, according to the NEHRP site classification based on the preferred $V_{s,30}$ values. The choice of selecting these soil conditions merely depends on the large number of records which is available for this type of soils (especially for the case of pulse-like records).

3. Intensity measures

The IMs under investigation from the literature are categorized into two groups: 1) non-structure-specific IMs, calculated directly from ground motion time histories; 2) structure-specific IMs, obtained from response spectra of ground motion time histories. The first group of IMs is further classified into three categories: acceleration-related, velocity-related and displacement-related IMs.

PGA (Peak Ground Acceleration), PGV (Peak Ground Velocity), PGD (Peak Ground Displacement), IV (Incremental Velocity), ID (Incremental Displacement), AI (Arias Intensity) are included in the first group. PGA, PGV and PGD are the most common time domain parameters of strong ground motions. PGA and PGV represent the peak of the acceleration and velocity time series, respectively. PGA has commonly been used to describe ground motions because of its natural relationship to inertial forces: indeed, the largest dynamic forces induced in certain types of structures (i.e. very stiff structures) are closely related to the PGA. Nevertheless, ground motions with high PGA are not necessarily more destructive than motions with lower PGA. Very high peak accelerations that last for only a very short period of time (i.e. high-frequency cycles) may cause little damage to many types of structures. With respect to PGA, PGV is less sensitive to the higher frequency content of the ground motion, and usually provides a more accurate indication of potential damage in those structures that are sensitive to the intermediate frequency content of the seismic loading. PGD, instead, is strongly depends on the low frequency content of the ground motion, and is therefore an appropriate predictor for low fundamental frequency buildings (e.g., tall buildings). IV is defined as the area under the maximum acceleration pulse, while ID is the area under the maximum velocity pulse. AI was proposed by [12], and accounts for duration and amplitude but does not reflect the frequency content of the ground motion. AI tends to overestimate the intensity of long duration motions with high amplitude and a broad range of frequency content.

CAV (Cumulative Absolute Velocity) is defined as the integral of the absolute value of the acceleration time series. It was proposed as a conservative predictor of earthquake damage threshold for nuclear power plants safe-shut-down. CAV can be considered as the summation of the velocity amplitudes during the time. This explains the name given to this IM. It is evident from its definition that the value of CAV increases with time until it reaches its maximum at t_f . Because of this, CAV includes the cumulative effect of ground motion duration. I_c (Characteristic Intensity) was proposed by [32]. $S_a(T)$ (5%-damped pseudo-acceleration spectral value at a specified period T) is widely used because of its efficiency

and the availability of many Ground Motion Prediction Equations. $E_{la}(T)$ and $E_{lr}(T)$ (5%-damped absolute and relative input energy spectral value, respectively) are structure-specific IMs defined in [33]. I_H (Housner Intensity) has been defined by [34] and it is related to the kinetic energy stored by the structure during the earthquake. Actually, I_H is defined as the integral of the pseudo-velocity spectrum within the interval 0.1s-0.25s, with the latter selected as representative of the periods of vibrations of civil engineering structures. ASI (Acceleration Spectral Intensity) has been proposed by [35] in order to select ground motions for the analysis of reinforced concrete dams, whose period of vibration typically ranges between 0.1s and 0.5s. Definition of I_a , I_v and I_d (Compound acc.-, vel.- and disp.-related IM, respectively) are given in [36]. References for FI (Fajfar Intensity), CAD (Cumulative Absolute Displacement), and SED (Specific Energy Density) can be found in [4].

4. Regression analysis

4.1 Predictive model

Several are the properties that are usually investigated for evaluating the predictive capabilities of an IM. The only property considered in this study is the efficiency.

An efficient IM is defined as one that yields relatively small variability of the predicted EDP for a given IM level. The efficiency can be evaluated by first running nonlinear dynamic analyses on the structure, and then by carrying out regression analyses between the obtained EDP values and the IM values of the used earthquake records. The standard error of the regression residuals σ_ϵ gives a direct measure of the IM efficiency.

It was observed by many researchers (e.g., [37]) that EDP-IM relationships, in general, typically follow a standard power law. This functional form is therefore used in the present study:

$$EDP = a \cdot (IM)^b \tag{1}$$

The equation above can be also expressed in the following logarithmic form:

$$\ln(EDP) = \ln(a) + b \cdot \ln(IM) \tag{2}$$

where $\ln(a)$ and b are model parameters to be determined by simple linear regression on $\ln(EDP)$ and $\ln(IM)$.

4.2 Results

Fig.7 and Fig.10 report the σ_ϵ values obtained in the regressions of the MIDR calculated for the structures isolated with the FPBs and the HDRBs, respectively. It is worth noting that in the HDRB case, the standard error of

residuals σ_ϵ is relatively large (i.e. greater than 0.4) for all the IMs. In this FPB case, instead, all the σ_ϵ values are lower than 0.40, with the most efficient predictors being the AI, I_c and ASI. In Fig.9 and Fig.12 the results of the IMs-MBD regressions are reported. It can be noticed that the trend in the efficiency of the IMs is similar for both structures, with σ_ϵ values being slightly larger in FPB case than in the HDRB case. The best predictors for this EDP are FI, SED, I_H and the spectral IMs S_a and E_{la} . Fig.8 and Fig.11 report the results of the IMs-MFA regressions. Also for this EDP, the trend in the efficiency of the IMs is similar for both structures. The difference with respect to the prediction of the MBD, is that in the HDRB case the errors are larger compared to those obtained in the FPB case. The most efficient predictors are the acceleration-related IMs PGA, I_a , I_c and ASI. In the FPB case, also AI can be considered as a good predictor.

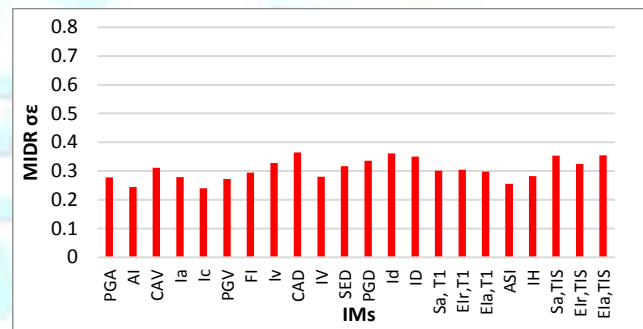


Fig.7 Standard error of residuals σ_ϵ obtained from the IMs-MIDR regression for the FPB-isolated building.

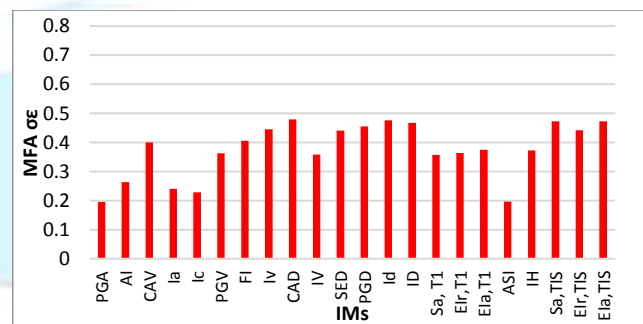


Fig.8 Standard error of residuals σ_ϵ obtained from the IMs-MFA regression for the FPB-isolated building.

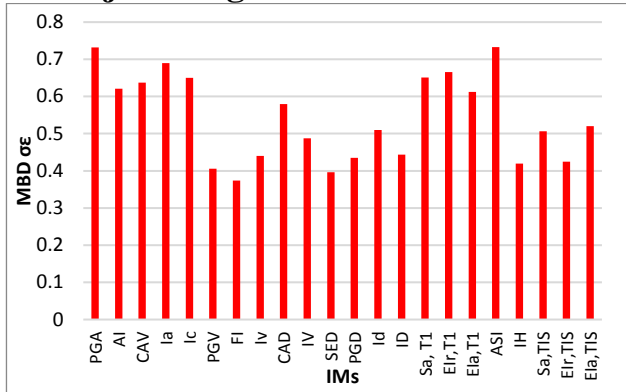


Fig.9 Standard error of residuals σ_ϵ obtained from the IMs-MBD regression for the FPB-isolated building.

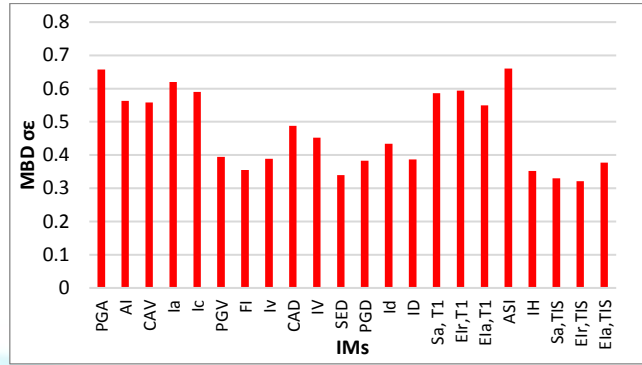


Fig.12 Standard error of residuals σ_ϵ obtained from the IMs-MBD regression for the HDRB-isolated building.

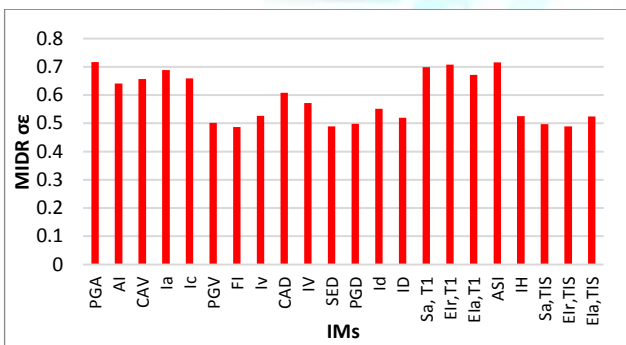


Fig.10 Standard error of residuals σ_ϵ obtained from the IMs-MIDR regression for the HDRB-isolated building.

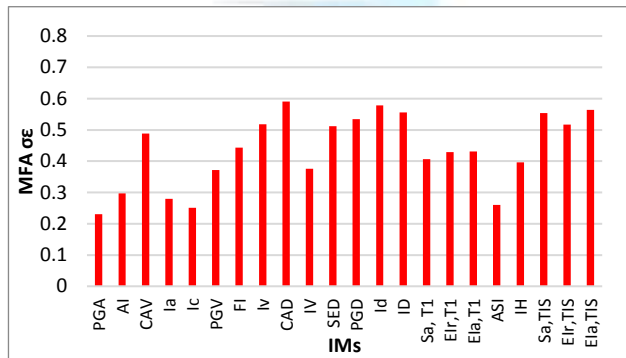


Fig.11 Standard error of residuals σ_ϵ obtained from the IMs-MFA regression for the HDRB-isolated building.

5. Conclusions

The aim of this work was to identify the IMs that better predict the seismic response of base-isolated buildings. To this end, a 6-storey RC frame building, designed for gravity loads only and then retrofitted by means of two different isolation systems, has been analyzed.

A set of 19 IMs has been selected, among the most widely used in the literature, and the following EDPs considered to measure seismic demand in the structures: Maximum Interstory Drift Ratios (MIDRs), Maximum Floor Accelerations (MFAs) and Maximum Base Displacement (MBD).

The predictive capability of the IMs was evaluated in terms of efficiency, and estimated through regression analyses of IM and EDP values obtained from a suite of 92 ground motion records.

The results have clearly shown that it is not possible to identify an optimal predictor for all the EDPs and for both the analyzed structures. In particular, the efficiency of the IMs change when the MIDR and MBD or the MFA is predicted. Among all the considered IMs, PGA and ASI have been found to be best predictors for MFA. About the prediction of the MIDR, a strong dependence of the efficiency of the IMs on the type of isolation system has been observed. In particular, higher values of the standard error σ_ϵ have been observed in the HDRB case than the FPB. In this latter case, the better IMs are AI, Ic and ASI as well. FI, has been found to be the best IM for the MBD prediction, together with the spectral IMs Sa, E1r and E1a.

References

[1] N. Shome, and C.A. Cornell, and P. Bassurro, and J.E. Carballo, "Earthquakes, records, and nonlinear responses", Earthq Spectra 14, 1998, pp. 469–500.

- [2] M. Bianchini, and P.P. Diotallevi, and J.W. Baker, "Prediction of inelastic structural response using an average of spectral accelerations", in 10th International Conference on Structural Safety and Reliability (ICOSSAR09), 13-17 September 2009, Osaka, Japan.
- [3] N. Jayaram, and F. Mollaioli, and P. Bazzurro, and A. De Sortis, and S. Bruno, "Prediction of structural response of reinforced concrete frames subjected to earthquake ground motions", 9th U.S. National and 10th Canadian Conference on Earthquake Engineering, pp. 428-437, 25-29 July 2010, Toronto, Canada.
- [4] F. Mollaioli, and A. Lucchini, and Y. Cheng, "Intensity measures for the seismic response prediction of base-isolated buildings", *Bulletin of Earthquake Engineering* 1, 2013, pp. 1841-1866.
- [5] N. Shome, and C.A. Cornell, "Probabilistic seismic demand analysis of nonlinear structures", RMS Program, Stanford University, Report No. RMS35 (1999) <https://blume.stanford.edu/rms-reports>. Accessed 2 June 2014.
- [6] N. Luco, and C.A. Cornell, "Structure-specific scalar intensity measures for near-source and ordinary earthquake ground motions", *Earthq Spectra* 23(2), 2007, pp. 357-392.
- [7] P.P. Cordova, and G.G. Deirlein, and S.S.F. Mehanny, and C.A. Cornell, "Development of a two-parameter seismic intensity measure and probabilistic assessment procedure" in: *Proceedings of the 2nd US-Japan workshop on performance-based earthquake engineering of reinforced concrete Building Structures*, 11-13 September 2000, Sapporo, Hokkaido, Japan.
- [8] L. Lin, and N. Naumoski, and N. Saatcioglu, and S. Foo, "Improved intensity measures for probabilistic seismic demand analysis", Part 1: development of improved intensity measures. *Can J Civ Eng* 38(1), 2011, pp. 79-88.
- [9] F. Mollaioli, and S. Bruno, and L. Decanini, and R. Saragoni, "Correlations between energy and displacement demands for performance-based seismic engineering", *Pure Appl Geophys* 168(1-2), 2011, pp. 237-259.
- [10] K.L. Ryan, and A.K. Chopra, "Estimation of seismic demands on isolators based on nonlinear analysis", *J Struct Eng* 130(3), 2004a, pp. 392-402
- [11] K.L. Ryan, and A.K. Chopra, "Estimating the seismic displacement of friction pendulum isolators based on nonlinear response history analysis", *Earthq Eng Struct Dyn* 33(3), 2004b, pp. 359-373
- [12] A. Arias, "A measure of earthquake intensity", *Seismic design for nuclear power plants*, R.J. Hansen ed. MIT, Cambridge, Mass, 1970, pp. 438-483
- [13] J.M. Nau, and W.J. Hall, "Scaling methods for earthquake spectra" *J Struct Eng* 110, 1984, pp. 1533-1548.
- [14] R. Araya, and G.R. Saragoni, "Capacidad de los movimientos de producir daño estructural", Publication SES I 7/80 (in Spanish), Division of Structural Engineering, Department of Engineering, University of Chile, Santiago, 1980.
- [15] L.F. Ibarra, and R.A. Medina, and H. Krawinkler, "Hysteretic models that incorporate strength and stiffness deterioration", *Earthquake Engineering and Structural Dynamics*, 34(12), 2005, pp. 1489-1511.
- [16] "OpenSees," University of California, 2000. [Online]. Available: [http://opensees.berkeley.edu/wiki/index.php/Modified_Ibarra-Medina-Krawinkler_Deterioration_Model_with_Pinched_Hysteretic_Response_\(ModIMKPinching_Material\)](http://opensees.berkeley.edu/wiki/index.php/Modified_Ibarra-Medina-Krawinkler_Deterioration_Model_with_Pinched_Hysteretic_Response_(ModIMKPinching_Material)) [Accessed 2017].
- [17] F. Braga, and R. Gigliotti, and M. Laterza, and M. D'Amato, and S.F. Kunnath, "Modified Steel Bar Model Incorporating Bond-Slip for Seismic Assessment of Concrete Structures", *J. Struct. Eng. ASCE*, 138, 2012, pp. 1342-1350.
- [18] G.M. Calvi, and G. Magenes, and S. Pampanin, "Relevance Of Beam-Column Joint Damage And Collapse In Rc Frame Assessment", *Journal of Earthquake Engineering*, 6:S1, 2002, pp. 75-100.
- [19] G. Fabbrocino, and G. M. Verderame, and G. Manfredi, and E. Cosenza, "Structural models of critical regions in old-type r.c. frames with smooth rebars", *Engineering Structures* 26, 2004, pp. 2137-2148.
- [20] L. Decanini, and F. Mollaioli, and A. Mura, and R. Saragoni, "Seismic performance of masonry infilled R/C frames", 13th WCEE, paper N0. 165, Vancouver, Canada, 2004.
- [21] D. Cardone, and G. Palermo, and M. Dolce, "Direct displacement-based design of buildings with different seismic isolation systems", *Journal of Earthquake Engineering*, Vol. 14 (2), DOI: 10.1080/13632460903086036, 2010, pp. 163-191.
- [22] M. Kumar, and A. Whittaker, and M. Constantinou, "An advanced numerical model of elastomeric seismic isolation bearings" *Earthquake Engineering & Structural Dynamics*, Published online, DOI: 10.1002/eqe.2431, 2014.
- [23] "OpenSees," University of California, 2000. [Online]. Available: <http://opensees.berkeley.edu/wiki/index.php/HDR> [Accessed 2017].
- [24] D.N. Grant, and G.L. Fenves, and A.S. Whittaker, "Bidirectional modeling of high-damping rubber bearings", *Journal of Earthquake Engineering*, 8(1), 2004, pp. 161-185.
- [25] M.C. Constantinou, and A. Mokha, and A. Reinhorn, "Teflon bearings in base isolation", II: modeling. *Journal of Earthquake Engineering*, 116(2), 1990, pp. 455-474.
- [26] D. Cardone, and G. Gesualdi, and P. Brancato, "Restoring capability of friction pendulum seismic isolation systems", *Bulletin of Earthquake Eng. [ISSN: 1570761X]*, Vol. 13(8), DOI: 10.1007/s10518-014-9719-5, 2015, pp. 2449-2480.
- [27] D. Cardone, and G. Gesualdi, and G. Perrone, "Cost-benefit analysis of alternative retrofit strategies for RC framed buildings", *Journal of Earthquake Engineering*, DOI: 10.1080/13632469.2017.1323041, 2017.
- [28] D. Cardone, and G. Perrone, "Damage and loss assessment of pre-70 RC frame buildings with FEMA P-58", *Journal of Earthquake Engineering*, Vol. 21, DOI: 10.1080/13632469.2016.1149893, 2017, pp. 23-61.
- [29] K. Sassun, and D. Cardone, and T. Sullivan, and P. Morandi, "Characterising the seismic performance of infill masonry", *Bulletin of New Zealand Society for Earthquake Engineering*, Vol. 49, No. 1, 2016, pp. 100-117.
- [30] Pacific Earthquake Engineering Research (PEER) (2005) Next Generation Attenuation (NGA) project. <http://peer.berkeley.edu/nga/>.

- [31] J.W. Baker, "Quantitative classification of near-fault ground motions using wavelet analysis", *Bull Seismol Soc Am* 97(5), 2007, pp. 1486–1501.
- [32] A.H.S. Ang, "Reliability bases for seismic safety assessment and design", *Proceedings, Fourth National Conference on Earthquake Engineering, EERI, Palm Springs, 1, 1990*, pp. 29-45.
- [33] C.M. Uang, and V.V. Bertero, "Evaluation of seismic energy in structures", *EarthqEngStructDyn* 19(1), 1990, pp. 77-90.
- [34] G.W. Housner, "Behaviour of structures during earthquake". *Journal of the Engineering Mechanics Division, ASCE* 1959: 85(4), 1959, pp. 109–129.
- [35] J. L. Von Thun, and L. H. Rochim, and G. A. Scott, and J. A. Wilson, "Earthquake ground motions for design and analysis of dams" *Earthquake Eng. Soil Dyn. II—Recent Advances in Ground-Motion Evaluation (GSP 20)*, ASCE, New York, 1988, pp. 463–481.
- [36] R. Riddell, and J. Garcia, "Hysteretic energy spectrum and damage control" *EarthqEngStructDyn* 30(12), 2001, pp. 1791–1816.
- [37] C.A. Cornell, and F. Jalayer, and R.O. Hamburger, D.A. Foutch, "Probabilistic Basis for 2000 SAC Federal Emergency Management Agency Steel Moment Frame Guidelines", *J StructEng* 128(4), 2002, pp. 526-533.

